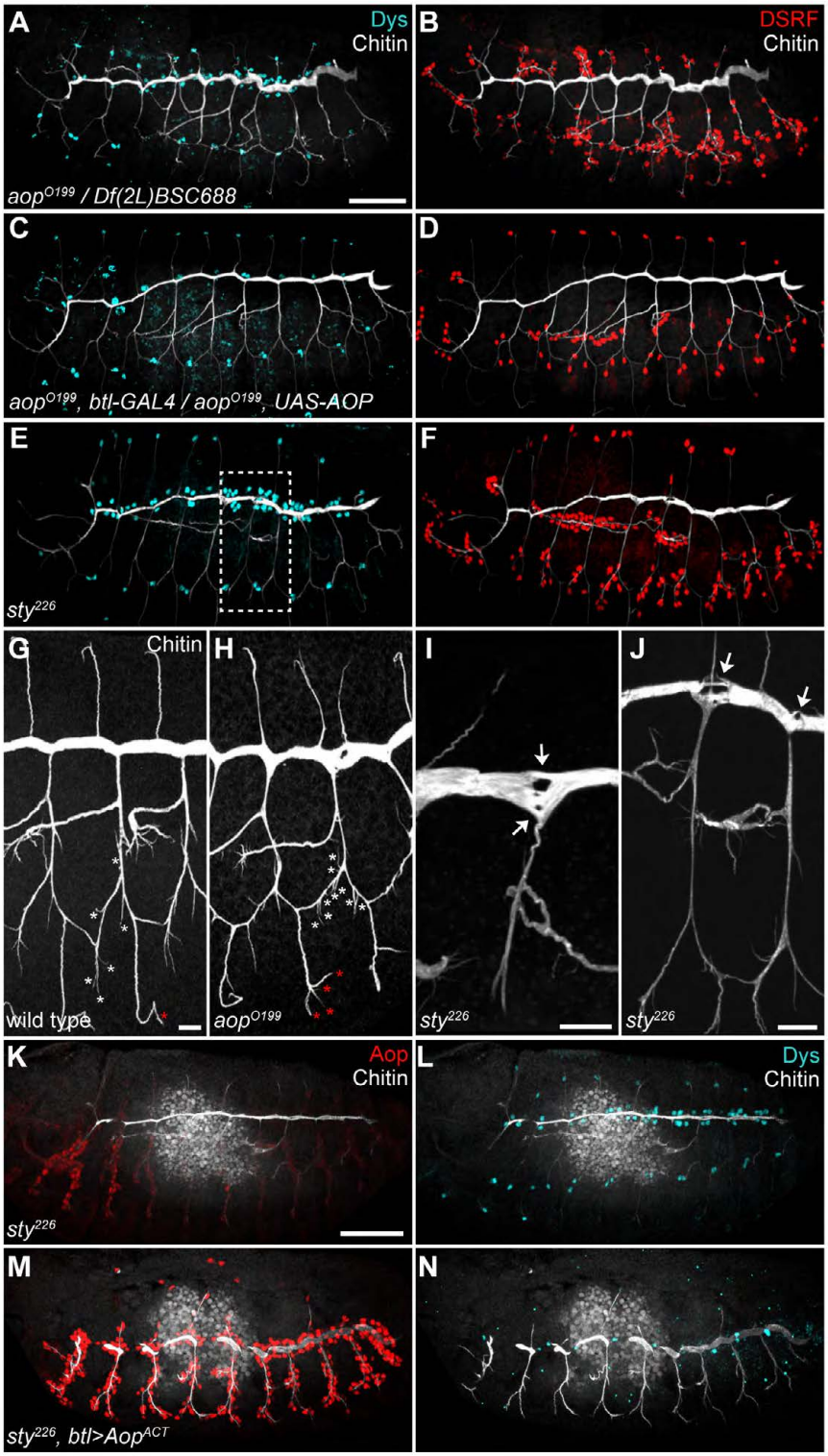

Fig. S1. *sty* mutants show similar mis-specification of fusion cells and terminal cells as *aop* mutants. (**A**,**B**) Stage 15-16 embryos stained for chitin (white), Dys (cyan, FCs) and DSRF (red, TCs). Hemizygous aop^{O199}/Df(2L)BSC688 embryos show defects resembling those of aop^{O199} homozygous embryos (see Fig. 2), indicating that aop^{O199} is an amorphic allele. (**C**,**D**) Tracheal-specific expression of *aop* under the control of *btl-GAL4* completely rescues the tracheal defects of aop^{O199} embryos, but does not rescue embryonic lethality and the head involution defect of aop^{O199} embryos (data not shown). Rescued embryos show normal numbers of FCs and TCs. (**E**,**F**) sty^{226} embryos show supernumerary FCs in the DT (E) and extra TCs in the remaining branches (F). (**G**,**H**) Higher magnifications of wild-type (G) and aop^{O199} (H) embryos stained for chitin show fine terminal branches in the lateral trunk (white asterisks) and in the ganglionic branch (red asterisks). Additional terminal branches are present in the aop^{O199} embryo. (I,J) Higher magnifications of the DT in sty^{226} embryos stained for chitin. The bifurcations in the DT lumen (arrows) resemble the *aop* phenotype (J is an enlargement of the area outlined in E). (K-N) Expression of Aop^{ACT} (detected by Aop antibody, red in M) in sty^{226} mutants suppresses ectopic FC specification in the DT in the absence of *sty* function (compare N with L). Scale bars: 50 µm in A-F,K-N; 10 µm in G-J.

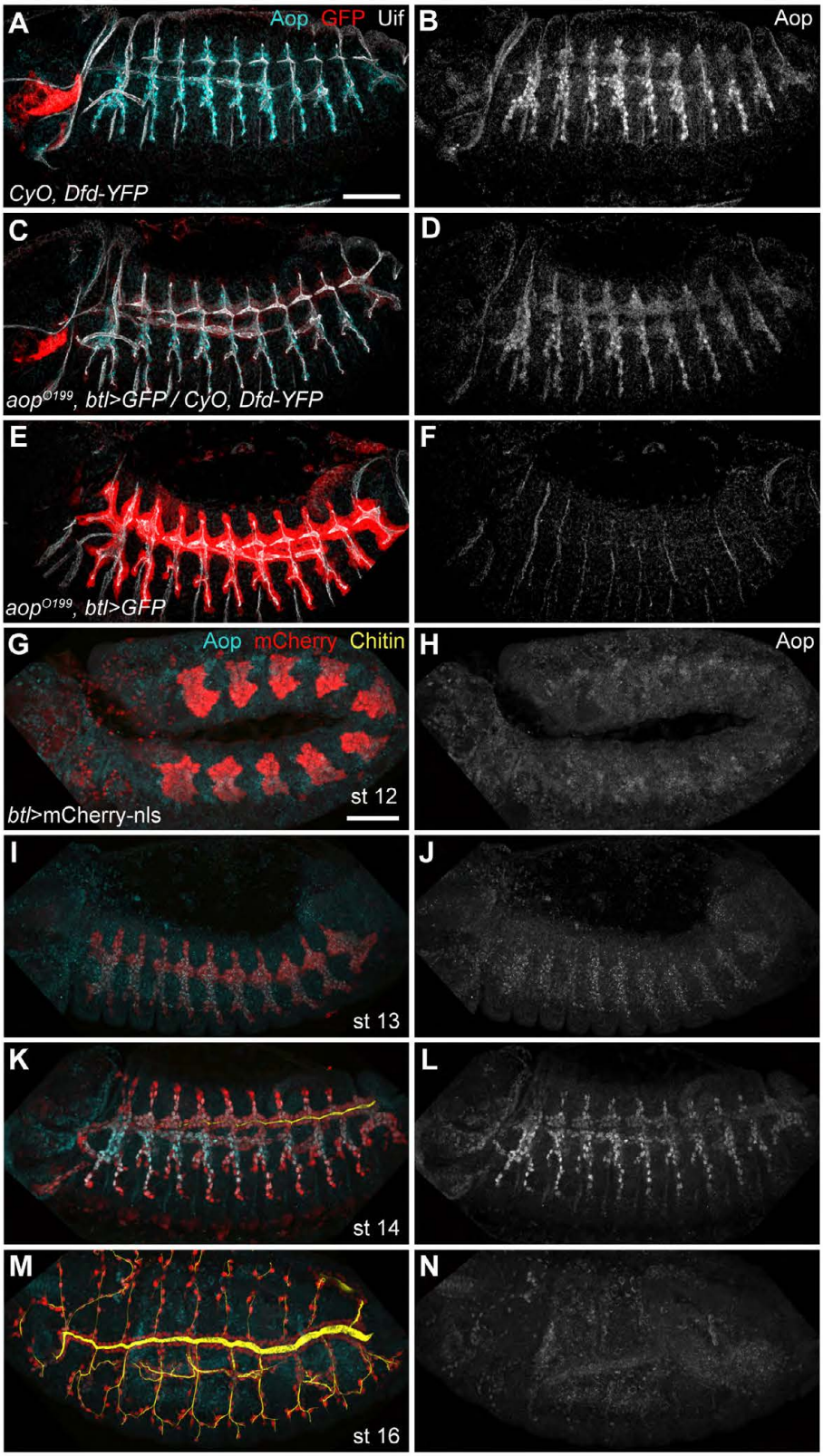

Fig. S2. Aop expression during tracheal development. (**A-F**) Stage 13 embryos from the parental genotype *aop^{O199} btl-Gal4 UAS-GFP UAS-Verm-mRFP/CyO Dfd-YFP* stained for GFP (red), Uninflatable (Uif; white) and Aop (cyan). No specific Aop signals are detected in *aop^{O199}* homozygous embryos (E,F). Sibling embryos homozygous (A,B) or heterozygous (C,D) for the *CyO Dfd-YFP* balancer chromosome were stained in the same reaction and imaged using the same settings as the *aop^{O199}* homozygous embryo. GFP signals in tracheal cells and Dfd-YFP signals in the head region were used to genotype embryos. The protein fragment used to raise the anti-Aop monoclonal antibody (Rebay and Rubin, 1995) includes, but is larger than, the predicted Aop[O199] truncated protein. Thus, lack of Aop staining in *aop^{O199}* embryos could be due to absence of the truncated protein or due to absence of the epitope from the truncated protein. (**G-N**) Stage 12 (G,H), stage 13 (I,J), stage 14 (K,L) and stage 16 (M,N) wild-type embryos expressing *mCherry-NLS* in all tracheal cells were stained for chitin (yellow), mCherry (red) and Aop (cyan). Aop becomes detectable in tracheal cell nuclei at stage 13 (I,J). Aop levels peak at stage 14 (K,L) and subsequently decline to low levels at 16 (M,N). Scale bars: 50 µm.

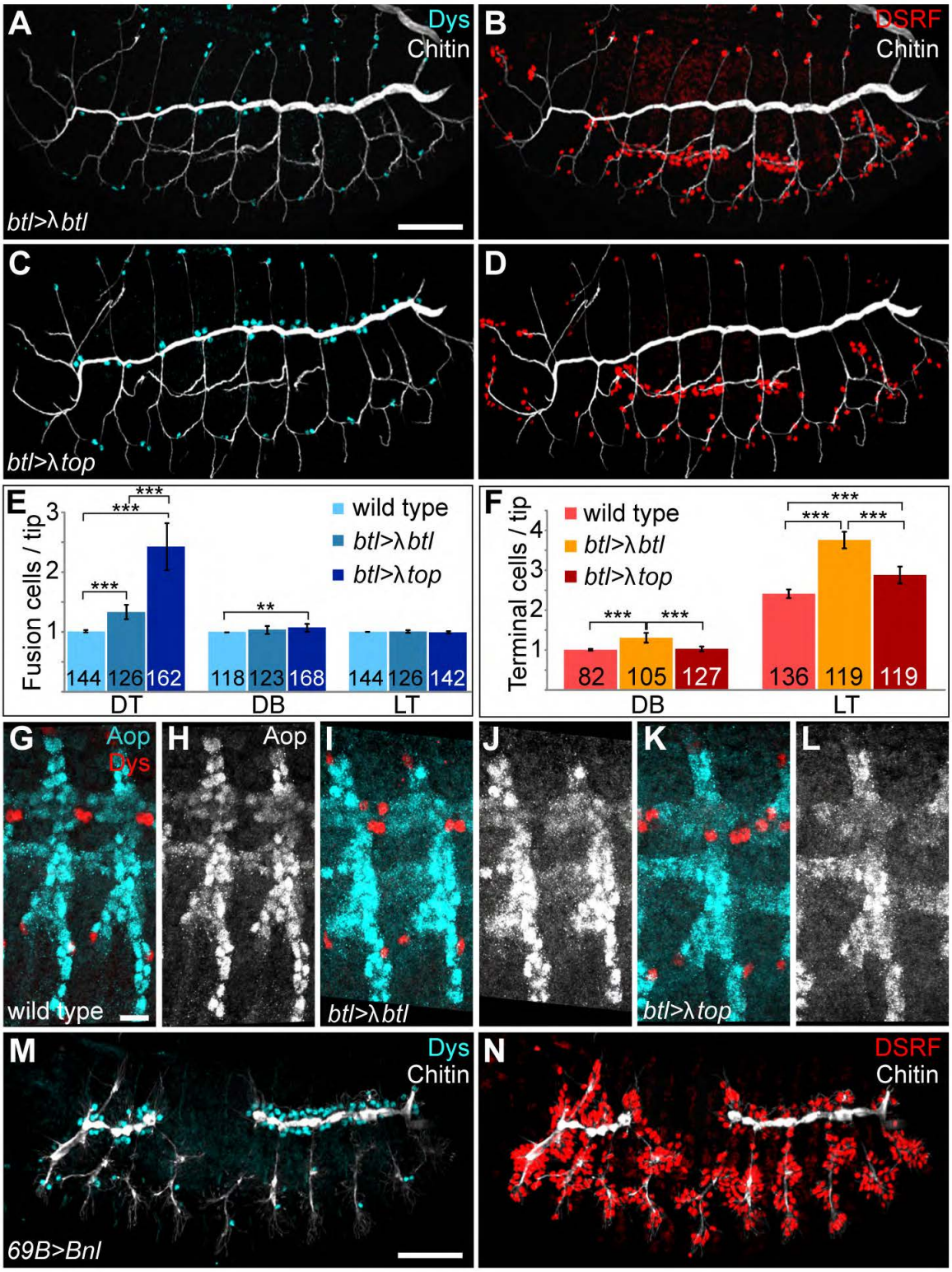

Fig. S3. Effect of constitutively active Receptor Tyrosine Kinase signaling on Aop levels in tracheal cells. (**A-F**) Constitutively active forms of Btl (λBtl; A,B) and EGFR (λTop; C,D) were expressed in tracheal cells under the control of *btl*-Gal4. The two receptors have distinct effects on FC and TC specification, respectively. FCs (E) and TCs (F) were counted in in λBtl- and λTop-expressing embryos. Branch types are indicated below the bars. Numbers inside bars indicate numbers of branch tips scored. Error bars represent s.d. ***$P \leq 0.001$; **$P \leq 0.01$. (**G-L**) Aop protein (cyan) was detected by immunostaining in wild-type embryos (G,H) and in embryos expressing λBtl (I,J) or λTop (K,L). Expression of λBtl and λTop leads to a partial downregulation of Aop in tracheal cells, probably owing to increased degradation (nuclear Aop signals are more diffuse in J and L compared with H). In λTop-expressing embryos (L), nuclear Aop signals in the DT are weaker compared with λBtl-expressing embryos (J), which is consistent with λTop being more potent than λBtl in inducing FCs. (**M**,**N**) Stage 15 embryo overexpressing Bnl in all ectodermal cells using the *69B*-Gal4 driver. Most tracheal cells are mis-specified as DSRF-expressing TCs (red; N), as previously reported, but DT cells are mis-specified mainly as Dys-expressing FCs (cyan; M). Scale bars: 50 µm in A-D,M,N; 10 µm in G-L.

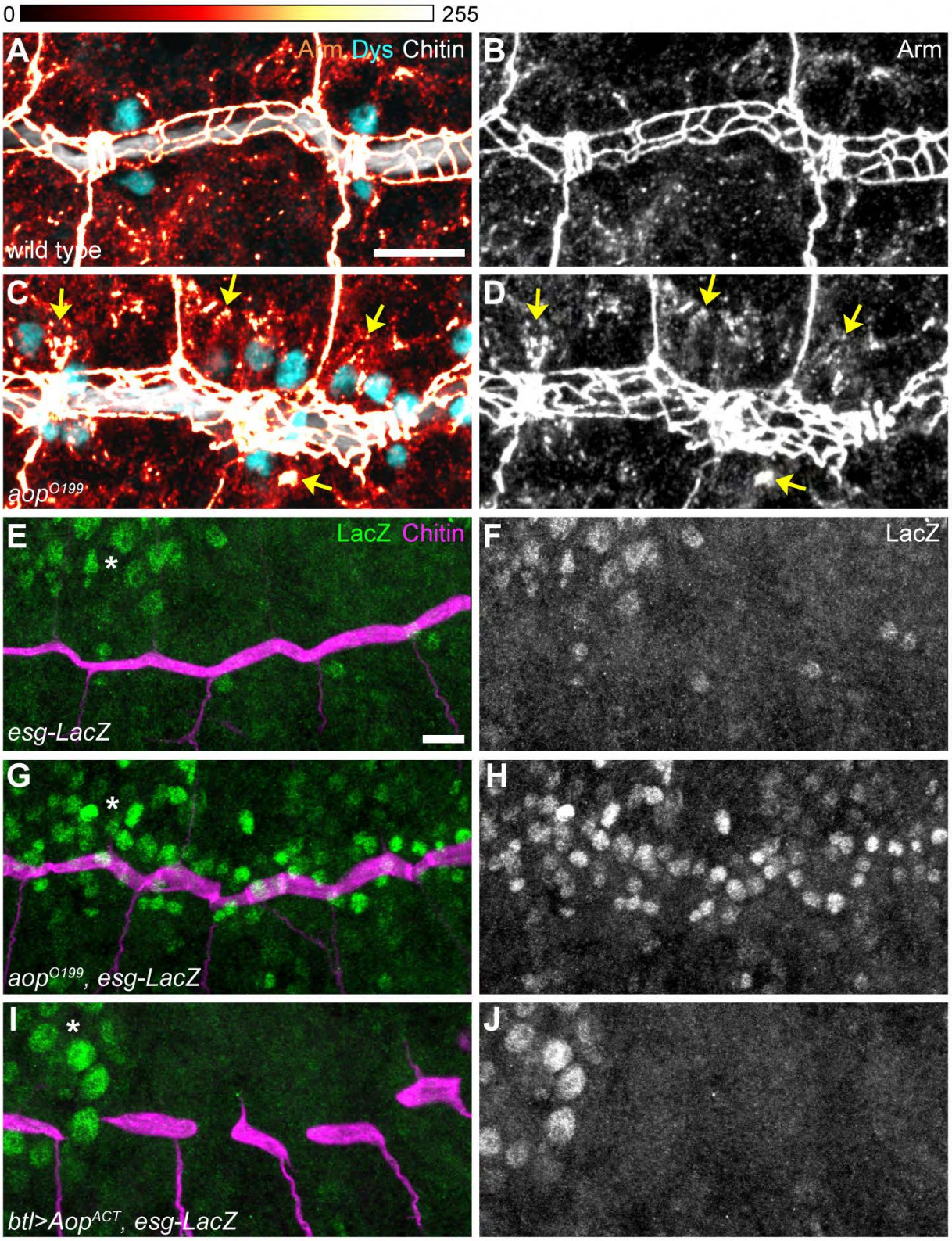

Fig. S4. *aop* mutations lead to accumulation of the Wg signaling effector Arm and to misexpression of the Wg target *escargot.* (**A-D**) Immunostaining showing Armadillo levels in wild-type (A, B) and aop^{O199} mutant embryo (C, D). aop^{O199} embryos show higher levels of intracellular Arm in DT cells compared to wild-type embryos. Also note patches of mislocalized Arm protein in ectopic FCs (C, D, yellow arrows). The images show maximum intensity projections of two sections (ΔZ=1.6 µm). Arm signal intensities in (A and C) are color-coded using a heat map shown on top. Note that Arm signals at AJs are saturated to highlight intracellular Arm signals. (**E-J**) *esg-LacZ* enhancer trap (green in E) reflects Wg-dependent expression of *esg* in two FCs per DT metamere in wild-type embryos (E,F). In aop^{O199} embryos (G,H), *esg-LacZ* is expressed in many more tracheal cells and at higher levels compared with wild-type embryos, consistent with overactivation of Wg signaling. Conversely, *esg-LacZ* is absent from tracheal cells expressing Aop^{ACT} (I,J). Non-tracheal cells expressing *esg-LacZ* are indicated by asterisks in E,G,I. Scale bars: 10 µm.

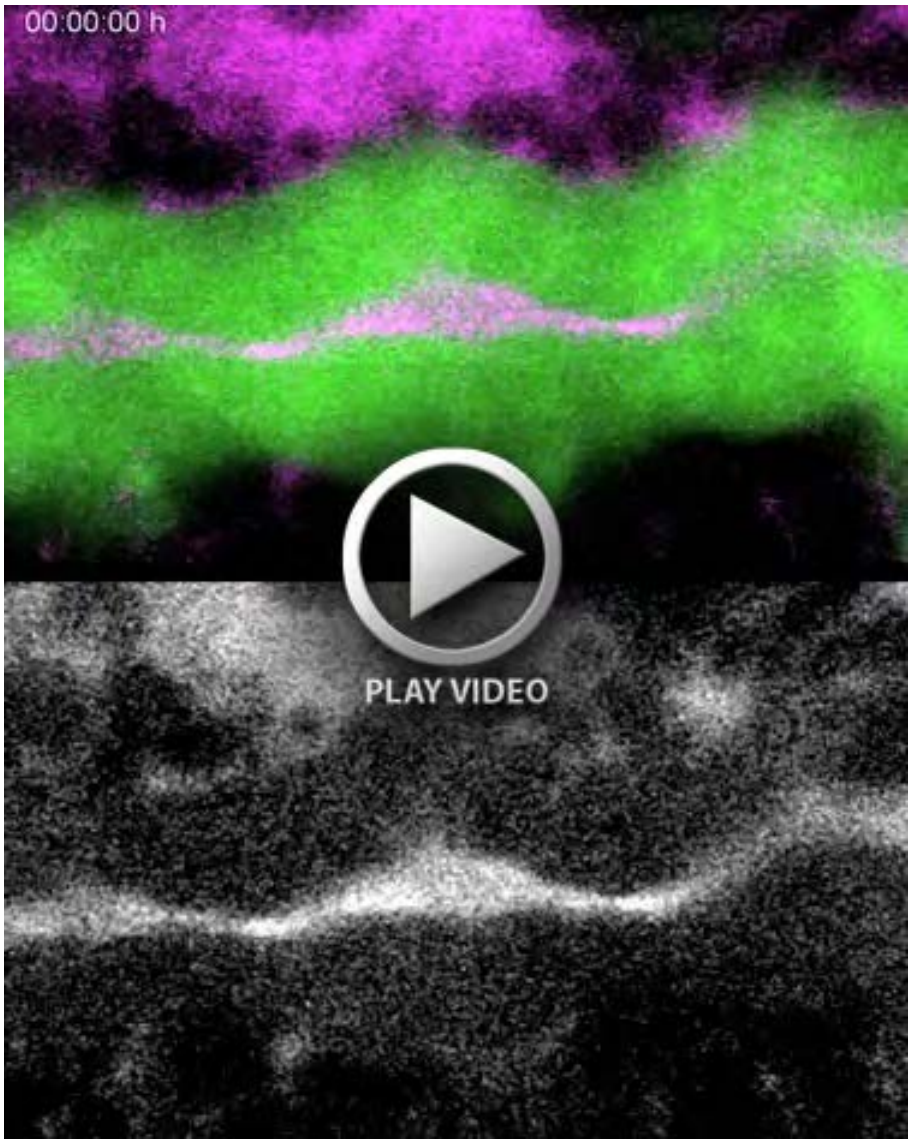

Movie 1. Ectopic tracheal fusion events in an *aop^{O199}* mutant embryo. Time-lapse movie of dorsal trunk in an *aop^{O199}* homozygous mutant embryo expressing GFP (green) and Verm-mRFP (magenta) under the control of *btl*-Gal4. The upper movie shows the merged GFP and Verm-mRFP channels and the lower movie shows the Verm-mRFP channel alone. Two separate cellular inclusions are formed in the DT lumen (green islets inside the lumen) owing to secondary fusion events. The movie was taken with a 40×/1.3 NA lens and a frame rate of 35 seconds. Time is indicated in the top left corner.